



UNICAMP

**UNIVERSIDADE ESTADUAL DE CAMPINAS
FACULDADE DE ODONTOLOGIA DE PIRACICABA**

JULIANA HADDAD

**COMPUTATIONAL ANALYSIS OF THE MECHANICAL BEHAVIOR OF
MANDIBULAR BONE STRUCTURES DURING THE MOLAR POWER
STROKE PHASE IN WISTAR RATS**

**ANÁLISE COMPUTACIONAL DO COMPORTAMENTO MECÂNICO
DAS ESTRUTURAS ÓSSEAS MANDIBULARES DURANTE A FASE DE
MORDIDA MOLAR EM RATOS DA LINHAGEM WISTAR**

JULIANA HADDAD

COMPUTATIONAL ANALYSIS OF THE MECHANICAL
BEHAVIOR OF MANDIBULAR BONE STRUCTURES DURING
THE MOLAR POWER STROKE PHASE IN WISTAR RATS

ANÁLISE COMPUTACIONAL DO COMPORTAMENTO
MECÂNICO DAS ESTRUTURAS ÓSSEAS MANDIBULARES
DURANTE A FASE DE MORDIDA MOLAR EM RATOS DA
LINHAGEM WISTAR

Tese apresentada à Faculdade de Odontologia de Piracicaba da Universidade Estadual de Campinas como parte dos requisitos exigidos para a obtenção do título de Doutora em Biologia Buco Dental, na Área de Anatomia.

Orientador: Prof. Dr. Alexandre Rodrigues Freire

ESTE EXEMPLAR CORRESPONDE A VERSÃO
FINAL DA TESE DEFENDIDA PELA ALUNA
JULIANA HADDAD ORIENTADA PELO PROF.
DR. ALEXANDRE RODRIGUES FREIRE.

Piracicaba
2022

Ficha catalográfica
Universidade Estadual de Campinas
Biblioteca da Faculdade de Odontologia de Piracicaba
Marilene Girello - CRB 8/6159

H117a Haddad, Juliana, 1991-
Análise computacional do comportamento mecânico das estruturas ósseas mandibulares durante a fase de mordida molar em ratos da linhagem Wistar / Juliana Haddad. – Piracicaba, SP : [s.n.], 2022.

Orientador: Alexandre Rodrigues Freire.
Tese (doutorado) – Universidade Estadual de Campinas, Faculdade de Odontologia de Piracicaba.

1. Ratos Wistar. 2. Método dos elementos finitos. 3. Mastigação. 4. Biomecânica. I. Freire, Alexandre Rodrigues, 1985-. II. Universidade Estadual de Campinas. Faculdade de Odontologia de Piracicaba. III. Título.

Informações Complementares

Título em outro idioma: Computational analysis of the mechanical behavior of mandibular bone structures during the molar power stroke phase in Wistar rats

Palavras-chave em inglês:

Rats, Wistar

Finite element method

Mastication

Biomechanics

Área de concentração: Anatomia

Titulação: Doutora em Biologia Buco-Dental

Banca examinadora:

Alexandre Rodrigues Freire [Orientador]

Talita Maximo Carreira Ribeiro

Fabiana Forti Sakabe

Luciane Ruiz Carmona Ferreira

Eduardo César Almada Santos

Data de defesa: 20-12-2022

Programa de Pós-Graduação: Biologia Buco-Dental

Identificação e informações acadêmicas do(a) aluno(a)

- ORCID do autor: <https://orcid.org/0000-0001-6356-8726>

- Currículo Lattes do autor: <https://lattes.cnpq.br/7404022484465527>



UNIVERSIDADE ESTADUAL DE CAMPINAS
Faculdade de Odontologia de Piracicaba

A Comissão Julgadora dos trabalhos de Defesa de Tese de Doutorado, em sessão pública realizada em 20 de dezembro de 2022, considerou a candidata JULIANA HADDAD aprovada.

PROF. DR. ALEXANDRE RODRIGUES FREIRE

PROF^a. DR^a. TALITA MAXIMO CARREIRA RIBEIRO

PROF^a. DR^a. FABIANA FORTI SAKABE

PROF^a. DR^a. LUCIANE RUIZ CARMONA FERREIRA

PROF. DR. EDUARDO CÉSAR ALMADA SANTOS

A Ata da defesa, assinada pelos membros da Comissão Examinadora, consta no SIGA/Sistema de Fluxo de Dissertação/Tese e na Secretaria do Programa da Unidade.

DEDICATÓRIA

Aos meus pais, Abib e Julia, por terem me ensinado as primeiras letras e por abdicado de suas vidas em prol das realizações e da felicidade de seus filhos.

Aos meus irmãos João (*in memoriam*) e Abib pelo carinho e incentivo.

À minha avó Maria (*in memoriam*) e Amélia, que desde os meus primeiros passos nunca me desampararam.

Ao meu namorado Leandro por todo amor, incentivo, apoio e compreensão. Nada disso teria sentido se vocês não existissem na minha vida.

AGRADECIMENTOS

À Universidade Estadual de Campinas, na pessoa do Magnífico Reitor Prof. Dr. Antônio José de Almeida Meirelles.

À Faculdade de Odontologia de Piracicaba, na pessoa do Senhor Diretor, Prof. Dr. Flávio Henrique Baggio Aguiar.

A Coordenadoria de Pós Graduação, na figura do Senhor Coordenador Prof. Dr. Valenrim Adelino Ricardo Barão.

À Equipe Técnica da Coordenadoria de Pós-graduação nas pessoas de Érica A. Pinho Sinhoreti, Raquel Q. Marcondes Cesar, Ana Paula Carone e Leandro Viganó agradeço pela paciência, atenção e disponibilidade em sempre me ajudar.

Aos servidores da biblioteca da FOP-UNICAMP pela valiosa disponibilidade e atenção.

O presente trabalho foi realizado com apoio da Coordenação de Aperfeiçoamento de Pessoal de Nível Superior – Brasil (CAPES) – Código de Financiamento 001.

Ao programa de pós-graduação em Biologia Buco-Dental, na figura da coordenador Prof. Dr. Marcelo Rocha Marques.

Ao meu orientador, Prof. Dr. Alexandre Rodrigues Freire, grande anatomista e amigo, pelos ensinamentos a mim transmitidos, pelo seu exemplo de ética e dedicação profissional. Por acreditar e valorizar a profissão acadêmica e confiar na minha capacidade, além de toda a paciência. Agradeço pela confiança, incentivo e oportunidades. Meu muito obrigada.

À professora Dr.^a Ana Cláudia Rossi, grande amiga, por ter sido não só companheira na orientação desse trabalho, mas em toda árdua caminhada. Sempre interessada no trabalho, oferecendo sugestões deveras muito importantes e a presença em todas as etapas para chegar até aqui. Jamais esquecerei muito obrigada.

Aos meus pais deixo um agradecimento especial pelo apoio incondicional e por todas as lições de amor, companheirismo, amizade e dedicação. Presentes em todos os momentos da minha vida, sendo meu alicerce desde que cheguei a este mundo, e mesmo quando achei que tudo tivesse acabado foram eles que me levantaram e mostraram que a vida é pra ser vivida mesmo com todos os acontecimentos nessa caminhada, que ainda está só começando. Obrigada por fazerem parte deste momento, sem vocês não teria chegado até aqui.

Aos meus irmãos Abib e João (*in memoriam*) que sempre acreditaram em mim, desde a graduação, embora o João tenha ido embora deste plano, sei que olha por mim e está sempre atorcida para que tudo dê certo na minha vida, e ao Abib meu agradecimento por ser a luz da minha vida, e mostrar que tudo vale a pena.

A minha avó Amélia e a madrinha Oneide por me oferecem o amor e a dedicação sem pedir nada em troca, apenas um sorriso.

Ao meu noivo Leandro, confiante e amigo, pelo incentivo e por permanecer ao meu lado foi muito importante nessa caminhada. Obrigada pelo presente de cada dia, pelo seu sorriso e por saber me fazer feliz.

As minhas amigas dessa caminhada, Luciane e Beatriz, obrigada pela amizade e carinho.

A aqueles que mesmo de forma direta e indireta colaboraram com este estudo.

RESUMO

O conhecimento da biomecânica do ciclo mastigatório do rato da linhagem Wistar é essencial para a interpretação dos resultados aplicados aos estudos dos processos fisiológicos envolvendo a remodelação óssea associada a mastigação. O objetivo deste estudo foi avaliar o comportamento mecânico da estrutura óssea mandibular de ratos da linhagem Wistar durante a fase de mordida molar no ciclo mastigatório pelo método dos elementos finitos. Os modelos de elementos finitos foram construídos a partir da segmentação de imagens de microCT da estrutura óssea do crânio de um rato Wistar macho de 3 meses de idade. A partir da segmentação, foram construídos os modelos tridimensionais da mandíbula, sínfise e os disco da articulação temporomandibular. A estimativa virtual da força muscular foi obtida pelo cálculo da área de secção-transversal. Como uma análise baseada nos conceitos do processo de mordida molar, durante o ciclo mastigatório, descrito por Weijs e Dantuma (1975), este ciclo é dividido em 6 fases, nas quais cada uma se caracteriza por atividade muscular e efeitos na estrutura óssea específicos. Assim, este estudo foi organizado em uma simulação caracterizada pela ação de uma força não-linear em 6 fases de mordida molar. Os resultados foram avaliados de acordo com os efeitos das variações das forças musculares em cada fase. O cálculo da deformação total do ramo da mandíbula foi realizado para avaliar as variações do ângulo entre os ramos da mandíbula e a posição do côndilo em cada fase. No geral, a deformação total da mandíbula apresentou configurações similares em todas as fases, com menores variações entre os lados. As deformações no corpo da mandíbula apresentaram direção inferior na região anterior aos molares e direção posterior na transição para o ramo da mandíbula. O ângulo entre os ramos da mandíbula diminuiu a partir da fase 1 até a fase 6. A posição do côndilo alterou para uma posição anterosuperior a partir da fase inicial. Conclui-se que os resultados apresentaram padrão biomecânico similar, na fase de mordida molar, de acordo com o descrito experimentalmente por Weijs e Dantuma (1975).

Palavras-Chave: rato, método dos elementos finitos, mastigação, biomecânica.

ABSTRACT

The chewing biomechanics knowledge of Wistar rat is essential to the result interpretation applied to the study of physiological process involving the bone remodeling associated with chewing. The aim was to evaluate the mechanical behavior of the bony structures of the mandible of Wistar rats during the molar power stroke phase in the bone structure, the variations in the angle between the mandibular rami and the position of the condyle from the mandibular deformation. The finite element models were built from the microCT image segmentation of the skull bone structure of a male and 3 months old Wistar rat. From the segmentation, a three-dimensional finite element model of the mandible, symphysis and temporomandibular disc were constructed. The estimated muscle force was initially obtained by calculating the muscle cross-sectional area. Based on the molar power stroke concept, described by Weijs and Dantuma (1975), this cycle is divided into 6 phases and each phase feature specific muscle activity and bony structure effects. Thus, this study was organized in a simulation, featured by a nonlinear force loading of 6 phases of the molar power stroke cycle. The results were evaluated according to the effects of muscle force variation in each phase. The calculation of the total deformation of the mandibular rami was performed to evaluate the variation in the angle of mandibular rami and the position of condyle in each phase. In overview, the total deformation of the mandible presented similar configurations in all phases, with minor variations between the sides. The deformations in the mandibular body showed inferior direction in the anterior region to the molars and posterior direction in the transition to the mandibular ramus. The angle between the mandibular rami decreased from the phase 1 to phase 6. The position of condyle changed to anterosuperior position from initial phase. In conclusion, the results presented similar biomechanical pattern in the power stroke phase, in accordance with the described experimentally by Weijs and Dantuma (1975).

Keywords: rat, finite element method, mastication, biomechanics.

SUMÁRIO

1	INTRODUÇÃO	10
2	ARTIGO: Computational analysis of the mechanical behavior of mandibular bone structures during the molar power stroke phase in wistar rats	14
3	CONCLUSÃO	34
	REFERÊNCIAS	35
	ANEXO 1: Comprovante de submissão na revista.....	37
	ANEXO 2: Comprovante do Comitê de Ética em Pesquisa.....	38
	ANEXO 3: Comprovante do software anti-plágio.....	39

1 INTRODUÇÃO

A mastigação tem sido avaliada em amplas pesquisas científicas, uma vez que este processo, assim como suas alterações, tem sido associado à manutenção do periodonto de suporte e a alterações no processo de remodelação óssea e nos tecidos dentais (Kaku et al., 2005). Nesta temática, pode-se encontrar estudos que utilizam diferentes espécies de animais para experimentos *in vivo* e, com isso, tornou-se importante a necessidade do entendimento dos processos fisiológicos destes animais, a fim de permitir uma melhor interpretação dos resultados experimentais e possibilitar uma relação com os processos da mastigação em humanos. Dentre as diferentes espécies de animais, as linhagens de ratos têm sido utilizadas e assim, no contexto da pesquisa aplicada ao processo da mastigação, diferentes ferramentas foram utilizadas para compreensão da mastigação nesta espécie (Weijs e Dantuma, 1975; Kaku et al., 2005; Cox et al. 2011, 2012; Ferreira et al., 2020; Rossi et al., 2021).

Hiemäe e Houston (1971) relataram que em mamíferos existem padrões básicos de movimentos mandibulares associados à alimentação, e que estes padrões influenciam a morfologia da dentição, a anatomia e a posição dos músculos da mastigação e a forma da articulação temporomandibular. Dentre os mamíferos, os roedores mostram provavelmente a mais extrema adaptação do aparelho da mastigação. Nos roedores, a incisão que é realizada pelos incisivos reduz o material antes da ingestão. A incisão é descrita de maneira separada da mastigação. Após a incisão, o material é transferido para os molares, onde ocorrerá a mastigação (Hiemäe e Ardran, 1968). Estes movimentos dependem diretamente de uma musculatura da mastigação especializada.

Weijs e Dantuma (1975) utilizaram a eletromiografia, assim como técnicas de imagens em cinemática, para entender o processo da mastigação em ratos da linhagem Wistar. Assim, determinaram 16 diferentes fases da mastigação, nas quais descreveram características da mandíbula e as variações de atividades muscular. As 16 fases da mastigação foram agrupadas

em 4 grandes ações do ciclo mastigatório, baseadas no estudo de Hiemäe e Ardran (1968), assim denominadas: (1) Mordida: realizada pela prensão dos incisivos; (2) Preparatória (mordida molar): transferência do alimento para a região dos molares e início do processo de trituração pelos molares; (3) Apertamento (molar): trituração pelo apertamento dos molares; e (4) Recuperação ou relaxamento: afastamento do molar caracterizado pelo relaxamento dos músculos da mastigação.

Cox et al. (2012) utilizaram o método dos elementos finitos (MEF) para entender as implicações biomecânicas que a morfologia do sistema da mastigação provoca em diferentes espécies de roedores. Os autores desenvolveram o modelo de elementos finitos de cada espécie através de microtomografias computadorizadas e, ainda, acrescentaram as informações a respeito dos músculos que atuam na mastigação, a saber, o músculo masseter superficial, as partes anterior e posterior do músculo masseter profundo, as partes anterior, posterior e infraorbital do músculo zigomático-mandibular, o músculo temporal e os músculos pterigoides interno e externo. Os autores relataram que o conhecimento da morfologia do crânio e dos músculos da mastigação permitiu identificar que os ratos apresentam alta performance tanto na fase de roer quanto na fase de triturar o alimento.

A caracterização do ciclo mastigatório foi um importante embasamento para pesquisas envolvendo a biomecânica craniofacial. As simulações computacionais pelo MEF proporcionaram a possibilidade de estimar parâmetros biomecânicos, como as forças musculares, forças de mordida e movimentos da mandíbula, que são considerados parâmetros de maior dificuldade de mensuração experimentalmente (Watson et al., 2014).

O uso do MEF associado à mastigação possibilitou avaliar a mecanobiologia do osso alveolar em situações de alteração oclusal, uma vez que nas simulações envolvendo a mordida e o apertamento dental é possível analisar as deformações ósseas associadas a mudanças no padrão mastigatório (Ferreira et al., 2020; Rossi et al., 2021).

Ferreira et al. (2020) utilizaram como modelo experimental uma alteração oclusal, através da extração dental (incisivo superior), e avaliaram sua influência na resposta do tecido ósseo alveolar do dente adjacente em ratos da linhagem Wistar. Os autores quantificaram os níveis de expressão da β -catenina e a deformação do osso alveolar por meio do MEF. Rossi et al. (2021) utilizaram como modelo experimental uma condição de contato prematuro no primeiro molar superior direito com o objetivo de avaliar a morfologia, a arquitetura e a remodelação óssea do osso alveolar da maxila de ratos da linhagem Wistar. Por meio da análise histológica, imunohistoquímica e pelo MEF, os autores avaliaram tridimensionalmente a microarquitetura óssea, a área da crista óssea alveolar, a expressão de RANK-L e TRAP e a distribuição de deformação equivalente e mínima principal da região do primeiro molar superior direito do rato. Para tanto, em ambos os estudos os autores desenvolveram um modelo tridimensional do crânio e da mandíbula do rato, tanto dos grupos controles quanto dos grupos experimentais para simular a mordida e conseguir quantificar as deformações mecânicas no osso alveolar. Os autores se atentaram à anatomia real do modelo, utilizando de conhecimentos obtidos em dissecções e em trabalhos como o de Cox et al. (2012) (Ferreira et al., 2020; Rossi et al., 2021).

Estes recentes estudos (Ferreira et al., 2020; Rossi et al., 2021) sugeriram que o melhor entendimento do ciclo da mastigação associado ao uso das simulações computacionais é fundamental para concluir os efeitos das alterações oclusais sobre os tecidos de suporte periodontal, importante temática pesquisada na Odontologia.

Com a evolução da simulação computacional associada à biomecânica craniofacial (Prado et al., 2013; Freire et al., 2014; Rossi et al., 2014; Prado et al., 2016), torna-se possível a aplicação dos conceitos e dados estabelecidos por Weijs e Dantuma (1975) referentes ao ciclo da mastigação de ratos, neste caso da linhagem Wistar. A necessidade do melhor entendimento

do ciclo da mastigação de ratos da linhagem Wistar, sugerida por pesquisas recentes (Ferreira et al., 2020; Rossi et al., 2021) reforça a necessidade do presente estudo.

Sendo assim, o presente estudo teve como objetivo avaliar o comportamento mecânico das estruturas ósseas da mandíbula de ratos da linhagem Wistar durante a fase de apertamento molar no ciclo da mastigação da estrutura óssea, as características das variações do ângulo entre os ramos da mandíbula e da posição da cabeça da mandíbula durante a fase de apertamento molar.

**2 ARTIGO: COMPUTATIONAL ANALYSIS OF THE MECHANICAL BEHAVIOR
OF MANDIBULAR BONE STRUCTURES DURING THE MOLAR POWER STROKE
PHASE IN WISTAR RATS***

*Artigo submetido para análise no periódico internacional: *Journal of Morphology*

(ANEXO 1)

ABSTRACT

The aim of this study was to evaluate the mechanical behavior of the bony structures of the mandible of Wistar rats during the molar power stroke phase of the chewing cycle, the characteristics of the variations in the angle between the rami of the mandible and the position of the mandibular condyle from the mandibular deformation during the molar power stroke phase. The finite element models were built from the microCT image segmentation of the bone structure of the skull of a male and 3 months old Wistar rat. From the segmentation of the microCT image, a three-dimensional surface of the mandible was constructed. The virtually estimated force is initially obtained by calculating the cross-sectional area. As it is an analysis based on the concept of the molar power stroke process, during the chewing cycle, described by Weijs and Dantuma (1975), this process has 6 phases, in which each one has characteristic muscular activities and characteristic effects on the bony structure. Thus, this study was organized in a simulation, featured by a nonlinear force loading of 6 phases of the molar power stroke cycle. The results were evaluated according to the effects of muscle forces during the power stroke. The calculation of the total deformation of the mandibular rami was performed, which presented the direction of the deformation and the amount of deformation in millimeters (mm). In an overview, the total deformation of the mandible presented similar configurations in all phases, with minor variations between the sides. The deformations in the mandibular body showed inferior direction in the anterior region to the molars and posterior direction in the transition to the mandibular ramus. The angle between the mandibular rami decreased from the phase 1 to phase 6. The position of condyle changed to anteriorsuperior position from initial phase. In conclusion, the results presented similar biomechanical pattern in the power stroke phase, in accordance with the described experimentally by Weijs and Dantuma (1975).

Keywords: rat, finite element method, mastication, rodent.

INTRODUCTION

Chewing has been evaluated in extensive scientific research, since this process, as well as its alterations, has been associated with the physiologic maintenance of the periodontium and changes in the bone remodeling process and dental tissues (Kaku et al., 2005). In this topic, studies that use different animal species for *in vivo* experiments and the need to figure out their physiological processes is important to obtain a better interpretation of experimental data and enable a relationship with masticatory knowledge applied to humans. Among the different species, the rat lineage has been used and thus, in the context of research applied to the chewing process, different tools have been used to understand the rat chewing process (Weijs and Dantuma, 1975; Kaku et al., 2005; Cox et al. 2011, 2012; Ferreira et al., 2020; Rossi et al., 2021).

Hiiemäe and Houston (1971) reported that in mammals there are basic patterns of mandibular movements associated with feeding, whose patterns influence the dentition morphology, the anatomy of the masticatory muscles and the shape of the temporomandibular joint (TMJ). Among mammals, rodents probably show the most extreme adaptation of the masticatory apparatus. In rodents, the incision made by the incisors reduces the material before ingestion. Incision is described separately from mastication. After the incision, the material is transferred to the molars, where chewing occurs (Hiiemäe and Ardran, 1968). These movements depend directly on a specialized group of masticatory muscles.

Weijs and Dantuma (1975) used electromyography, as well as kinematic imaging techniques, to figure out the chewing process in Wistar rats. Thus, they described 16 different phases of chewing, in which they described the pattern of mandible response associated with the variations in muscle activity. The 16 phases of mastication were grouped into 4 major phases of the chewing cycle, based on the study by Hiiemäe and Ardran (1968), as follows: (1) Biting: performed by gripping the incisors; (2) Preparatory stroke: transfer of food to the molar region

and initial grinding process by the molars; (3) Power stroke: grinding by clenching of molars; and (4) Recovery stroke: removal of the molar characterized by relaxation of the masticatory muscles.

Cox et al. (2012) used the finite element method (FEM) to understand the biomechanical implications in morphology of the masticatory system of different rodents. The authors developed a finite element model through microCT scans and added information about the masticatory muscles, involving the superficial masseter muscle, the anterior and posterior parts of the deep masseter muscle, the anterior, posterior and infraorbital parts of the zygomaticomandibularis muscle, the temporalis muscle and the internal and external pterygoid muscles. The authors reported that the knowledge of the skull morphology and the masticatory muscles allowed to identify that rats present high performance both in the gnawing (incisor biting) and phase of grinding.

The characterization of the masticatory cycle was an important basis for research involving craniofacial biomechanics. Computational simulations using FEM provided the possibility to estimate biomechanical parameters, such as muscle forces, bite forces, mandible bone stress, strain, deformation and movements, which are considered parameters that are more difficult to measure experimentally (Watson et al., 2014). The use of FEM associated with chewing have also allowed to evaluate the alveolar bone mechanobiology in situations of occlusal alteration, since in the simulations involving biting and power stroke are possible to analyze the bony deformations associated with changes in the masticatory pattern (Ferreira et al., 2020; Rossi et al., 2021).

Ferreira et al. (2020) used an occlusal alteration as an experimental model, through dental extraction (upper incisor), and evaluated its influence on the response of the alveolar bone tissue of the adjacent tooth in Wistar rats. The authors quantified protein expression levels associated to the alveolar bone deformation using the FEM. Rossi et al. (2021) used as

experimental rat model a condition of premature contact in the right maxillary first molar in order to evaluate the morphology, architecture and bone remodeling of the maxillary alveolar bone of Wistar rats. These recent studies (Ferreira et al., 2020; Rossi et al., 2021) have suggested that a better understanding of the rat chewing cycle, associated with the use of computational simulations, is essential to conclude the interpretation of effects by occlusal changes on periodontal support tissues.

The present study proposed the use of *in vivo* data from previous study (percentage of muscle contraction from electromyographic data) (Weijs and Dantuma, 1975) to make a more realistic computational model. Therefore, the aim of this study was to evaluate the mechanical behavior of the bony structures of the mandible of Wistar rats during the molar power stroke phase of the chewing cycle, the characteristics of the variations in the angle between the rami (AR) of the mandible and the position of the mandibular condyle (PC) from the deformation during the molar power stroke phase.

MATERIALS AND METHODS

This study used microtomographic images that had already been obtained in previous research in the original protocol (CEUA/UNICAMP protocol – number 4401-1), with no *in vivo* manipulation. Therefore, the Ethics Committee on the Use of Animals at UNICAMP – CEUA/UNICAMP exempted the present study from a new evaluation, considering it approved (ANEXO 2).

Sample and Construction of finite element models

The finite element models were built from the microCT image segmentation of the bone structure of the skull of a male and 3 months old Wistar rat from the Multidisciplinary Center for Biological Investigation on Laboratory Animal Center – CEMIB-UNICAMP. All

procedures were performed according to national legislation enforced by the National Council of Animal Experimentation Control (CONCEA) of Brazil. The euthanasia was performed by anesthesia overdose (pentobarbital sodium, 100 mg/kg). The head was disjointed from the body and fixed in 10% formalin solution and 0.1 M phosphate buffer (pH 7.4) for 24h at 4 °C. Then, the head was scanned in a SkyScan 1174 microtomography (Bruker, Kontich, Belgium), configured with 500 μ A current and 50 kV peak voltage.

From the segmentation of the microCT image, a three-dimensional surface of the mandible was constructed, which was optimized and converted into a volumetric model composed by tetrahedral elements (Figure 1). In addition to the bone structure, to better reproduce the effects of muscle forces on the mandible, a model of the temporomandibular joint (TMJ) disc and the connective tissue of symphysis were also constructed from the microCT image.

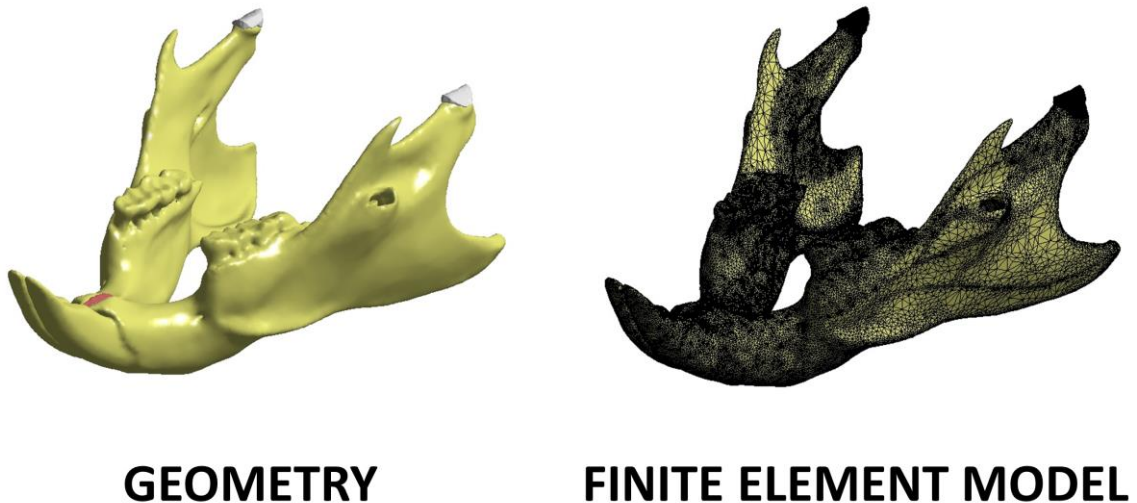


Figure 1. Three-dimensional geometry and finite element model composed by tetrahedral elements of mandible (yellow), symphysis (red) and TMJ disc (light grey).

Estimated calculation of muscle strength and orientation

Previous studies have presented computational simulations with muscle action from the calculation of muscle action force determined experimentally (Cox et al. 2011, 2012; Watson et al., 2014) and virtually (Humphries et al., 2021). When performed virtually, the value is estimated, since the calculation involves the average value of muscle fiber length (Humphries et al., 2021). The virtually estimated force is initially obtained by calculating the cross-sectional area (CSA). To obtain the CSA values, the following formula must be used:

$$CSA = \frac{Vm}{Lf}$$

where CSA is the cross-sectional area (in cm²), Vm is the muscle volume (in cm³) and Lf is the average length of muscle fiber (in cm).

Muscle volumes (Table 1) were obtained from the segmentation of contrast-enhanced microtomography images, performed in a previous study (Haddad, 2018). From the muscle location, the average fiber length of each muscle was estimated through the distance from the origin to the insertion (Table 2). Obtaining the CSA values for each muscle (Table 3), the maximum estimated force value (Table 4) was obtained by multiplying the CSA values by the muscle tension value equal to 22.5 N/cm² (Humphries et al., 2021).

Muscle force orientation was obtained using Rhinoceros 3D 5.0 software (McNeel & Associates, Seattle, USA) through lines representing the connection of the central positions of the origin and insertion sites of each muscle. From the lines, the x, y and z components of each muscle force were determined.

Table 1. Virtual muscle volumes of Wistar rat from 3D reconstruction of contrast-enhanced microCT.

MUSCLE VOLUME (cm³)			
RIGHT SIDE	VALUES	LEFT SIDE	VALUE S
Temporalis	0.301	Temporalis	0.301
Superficial Masseter	0.305	Superficial Masseter	0.305
Deep Masseter	0.507	Deep Masseter	0.507
Orbital Zygomaticomandibularis	0.017	Orbital Zygomaticomandibularis	0.017
Anterior Zygomaticomandibularis	0.073	Anterior Zygomaticomandibularis	0.073
Posterior Zygomaticomandibularis	0.023	Posterior Zygomaticomandibularis	0.027
Internal Pterygoid	0.126	Internal Pterygoid	0.126
External Pterygoid	0.047	External Pterygoid	0.047

Table 2. Muscle fiber length of Wistar rat from 3D reconstruction of contrast-enhanced microCT.

MUSCLE FIBER LENGTH (cm)			
RIGHT SIDE	VALUES	LEFT SIDE	VALUE S
Temporalis	1.9144	Temporalis	1.8430
Superficial Masseter	2.4407	Superficial Masseter	2.4679
Deep Masseter	2.8116	Deep Masseter	2.8323
Orbital Zygomaticomandibularis	1.1267	Orbital Zygomaticomandibularis	1.1315
Anterior Zygomaticomandibularis	1.4867	Anterior Zygomaticomandibularis	1.4884
Posterior Zygomaticomandibularis	1.1661	Posterior Zygomaticomandibularis	1.2334
Internal Pterygoid	1.0399	Internal Pterygoid	1.0366
External Pterygoid	0.9294	External Pterygoid	0.9375

Table 3. Values of CSA calculation from masticatory muscle parameters of Wistar rat.

CSA – CROSS-SECTIONAL AREA (cm²)			
RIGHT SIDE	VALUES	LEFT SIDE	VALUE S
Temporalis	0.1576	Temporalis	0.1637
Superficial Masseter	0.1253	Superficial Masseter	0.1241
Deep Masseter	0.1806	Deep Masseter	0.1793
Orbital Zygomaticomandibularis	0.1545	Orbital Zygomaticomandibularis	0.0153
Anterior Zygomaticomandibularis	0.0495	Anterior Zygomaticomandibularis	0.0495
Posterior Zygomaticomandibularis	0.0199	Posterior Zygomaticomandibularis	0.0219
Internal Pterygoid	0.1219	Internal Pterygoid	0.1223
External Pterygoid	0.0506	External Pterygoid	0.0502

Table 4. Maximum estimated muscle force of masticatory muscle of Wistar rat.

ESTIMATED MUSCLE FORCE (TOTAL - 100%, IN NEWTONS)			
RIGHT SIDE	VALUES	LEFT SIDE	VALUES
Temporalis	3.546	Temporalis	3.6832
Superficial Masseter	2.8192	Superficial Masseter	2.7922
Deep Masseter	4.0635	Deep Masseter	4.0342
Orbital Zygomaticomandibularis	3.4762	Orbital Zygomaticomandibularis	0.3442
Anterior Zygomaticomandibularis	1.1137	Anterior Zygomaticomandibularis	1.1137
Posterior Zygomaticomandibularis	0.4477	Posterior Zygomaticomandibularis	0.4927
Internal Pterygoid	2.7427	Internal Pterygoid	2.7517
External Pterygoid	1.1385	External Pterygoid	1.1295

According to the study performed by Weijs and Dantuma (1975), each phase of the masticatory cycle is characterized by the percentage of action of each muscle, whose data were obtained by electromyography. Thus, in each of the 6 phases proposed in this study, the percentages were applied to the maximum estimated force values.

Simulation by finite element analysis

As it is an analysis based on the concept of the molar power stroke process, during the chewing cycle, described by Weijs and Dantuma (1975), this process has 6 phases, in which each one has characteristic muscular activities and characteristic effects on the bony structure. Thus, this study was organized in a simulation, featured by a nonlinear force loading of 6 phases of the molar power stroke cycle.

The phases 1 to 4 show the maximum muscular activity value in the power stroke of the superficial masseter. The phases 4 and 5 show that all portions of the masseter and the posterior temporal muscle rapidly diminishes. The phase 6 comprises the opening movement, in which all portions of the temporal muscle are silent (Weijs and Dantuma, 1975).

Analyzes were performed using Ansys Workbench Structural Mechanics v17.2 software (Ansys Inc. Canonsburg, USA). The finite element models were imported and

assigned according to the mechanical properties. All the structures were considered as linear elastic and isotropic material. The mandible was assigned as bone structure with elastic modulus $E = 19,620$ MPa and Poisson's ratio $\nu = 0.3$ (Cox et al., 2012). The symphysis was assigned as connective tissue with elastic modulus $E = 50$ MPa and Poisson's ratio $\nu = 0.4$ (Cox et al., 2012) and the TMJ disc was assigned as fibrocartilage with elastic modulus $E = 44.1$ MPa and Poisson's ratio $\nu = 0.4$ (Tanaka et al., 2001).

For the boundary condition, the nodes of the superior surface on the disc were fixed in the medial-lateral axis and considered free in the antero-posterior and superior-inferior axes. For the loading condition, the values of the estimated muscular forces of each muscle were applied in their respective areas of insertion (Figure 2), which were determined by the visualization of the three-dimensional surfaces of the muscles. The values were applied corresponding to each force component (axes), characterizing the direction of muscle contraction. The forces were applied following the estimated value in each phase, featuring a nonlinear loading divided into the six phases.

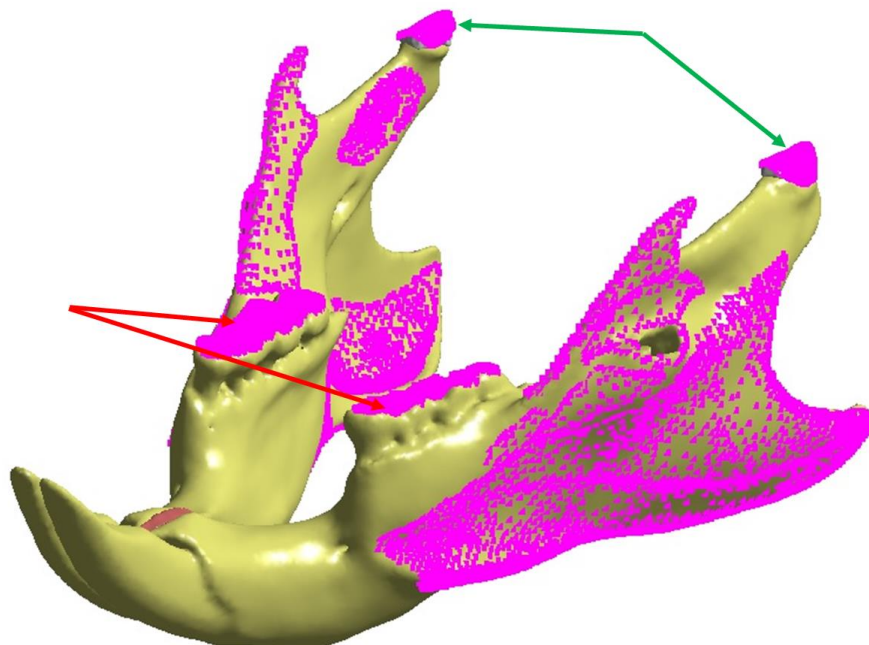


Figure 2. Analysis configuration including the load and boundary conditions. The load condition is indicated by the pink nodes on each muscle insertion area. The boundary conditions

are indicated by the pink nodes on the occlusal surface of lower molars (red arrows) and the superior surface of TMJ disc (green arrows).

Data analysis

The results were evaluated according to the effects of muscle forces during the power stroke on the AR and PC parameters, whose data were described by Weijjs and Dantuma (1975), featuring a large or small AR and anterior or posterior PC. For both parameters, the calculation of the total deformation (TD) of the mandibular rami was performed, which presented the direction of the deformation and the amount of deformation in millimeters (mm). From images by inferior view of TD in each phase (Figure 3), the AR value was obtained using ImageJ v1.53 software (National Institutes of Health, USA). To obtain the AR value, the sides of the angle were considered by a line from the right and left angular processes to the contact point between the lower incisors (Figure 4). The contact point between the incisors was considered the vertex of the angle. The AR values were compared from the initial model (no muscle action) to the last phase (Phase 6).

The PC was evaluated from the effect of the TD on mandibular rami and, consequently, on the condyles. From medial view images of the 6 phases on the right and left sides, the highest point of the articular condyle surface curvature was considered as a position reference. The images of each phase were placed in superposition to compare the positions of each reference point of the condyle (Figures 5 and 6).

RESULTS

In an overview, the TD (Figure 3) of the mandible presented similar configurations in all phases, with minor variations between the sides. The deformations in the mandibular body showed inferior direction in the anterior region to the molars and posterior direction in the transition to the mandibular ramus. In the mandibular ramus, the TD presented different patterns

in the angular process, coronoid process, and condyle. In the phases 1 and 2, the angular process presented deformation toward posterior direction and in the phases 3 to 6, the deformation presented medial direction. In all phases, the coronoid process showed deformation toward medial direction. The condyle showed deformation toward superior and anterior directions in all phases.

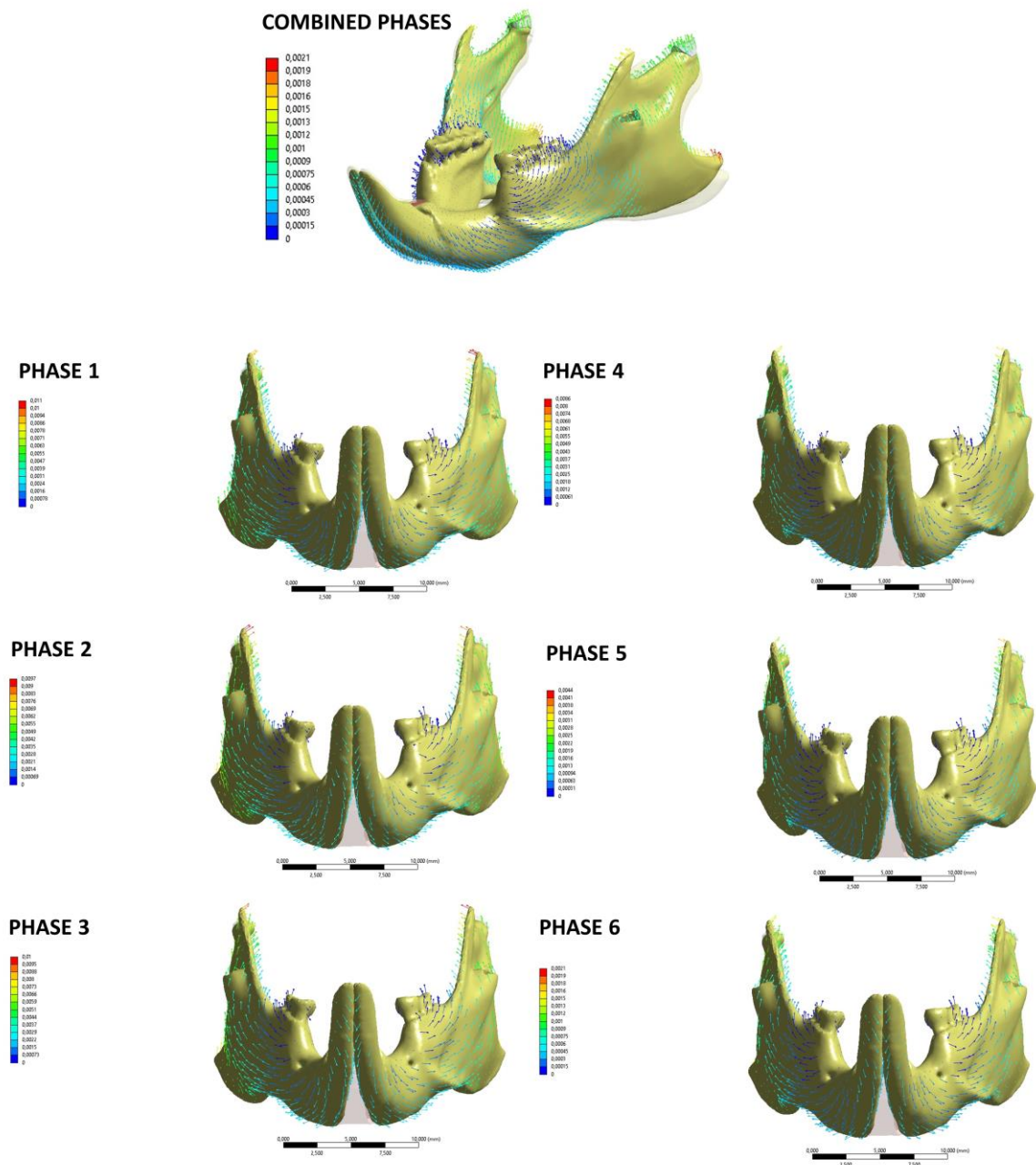


Figure 3. Total deformation configurations of the combined phases (anterolateral view) and in each phase of power stroke cycle (anterior view).

The AR value showed changes according to the power stroke phases. From the muscular actions in the phase 1, the angle presented minor decrease to the phase 3. From the phase 4, the AR values presented major decrease, finishing with a smaller angle in the last phase (Table 5).

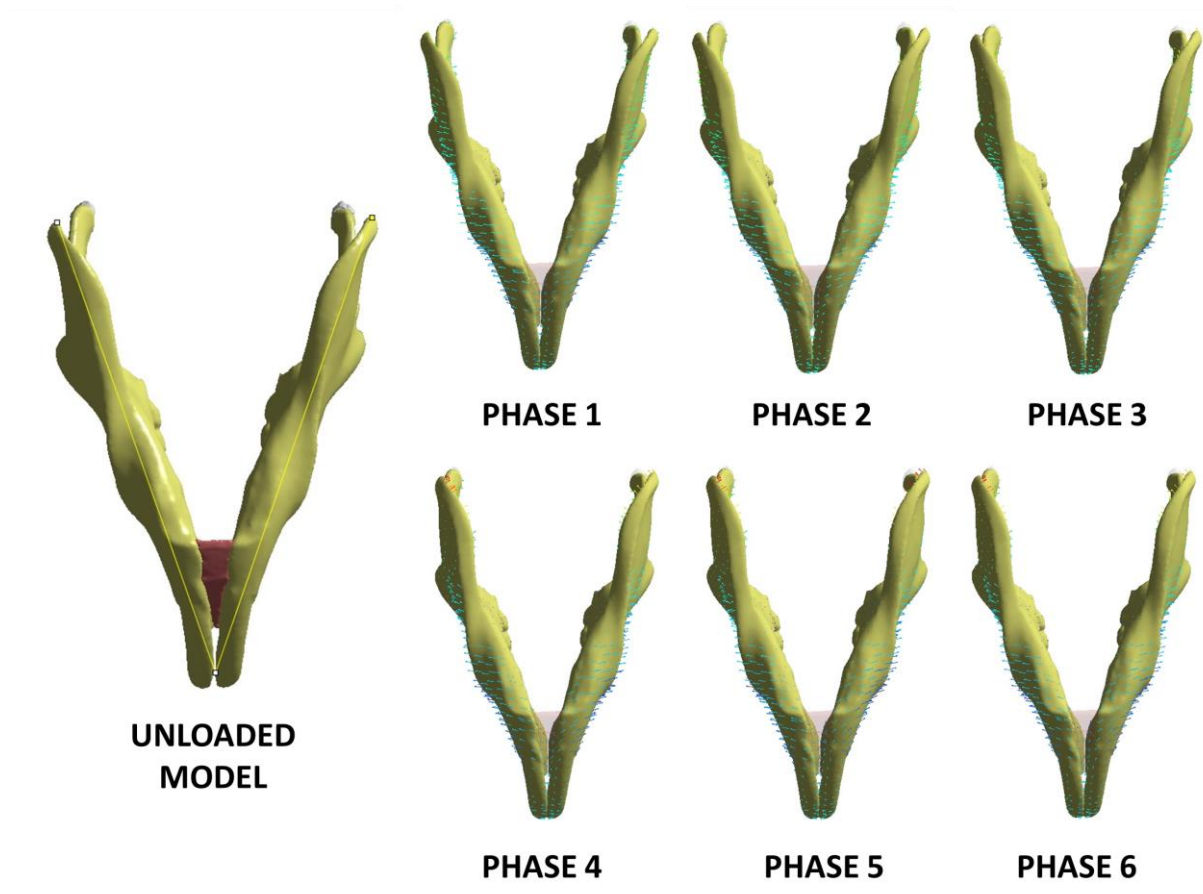


Figure 4. Inferior view of the models in the unloaded phase and the six phases of the power stroke cycle. The yellow line in the unloaded model indicates the angle between the mandibular rami.

Table 5. Values of angle between the mandibular rami in the unloaded model (initial condition) and the six phases of power stroke cycle.

PHASES	VALUES
Unloaded model	38.41
Phase 1	36.93
Phase 2	36.87
Phase 3	35.82
Phase 4	34.55
Phase 5	34.09
Phase 6	34.55

The PC was evaluated from the initial position (without muscle action). From the initial position, the condyle presented superior and anterior position, featuring minor variations in each phase. On the right side (Figure 5), the condyle was positioned superiorly and anteriorly in phase 1, 2, 3 and 4. In phases 5 and 6, the position was posterior in relation to the previous phases but maintained a superior and anterior position from the initial position. On the left side (Figure 6), the condyle presented superior and anterior position in phase 1 and 2. In the phase 3, the condyle positioned posteriorly and inferiorly in relation to phase 2. In the phase 4, the deformation resulted in anterior and superior position in relation to phase 3 and in the phases 5 and 6, the condyle presented posterior and inferior position in relation to phase 4.

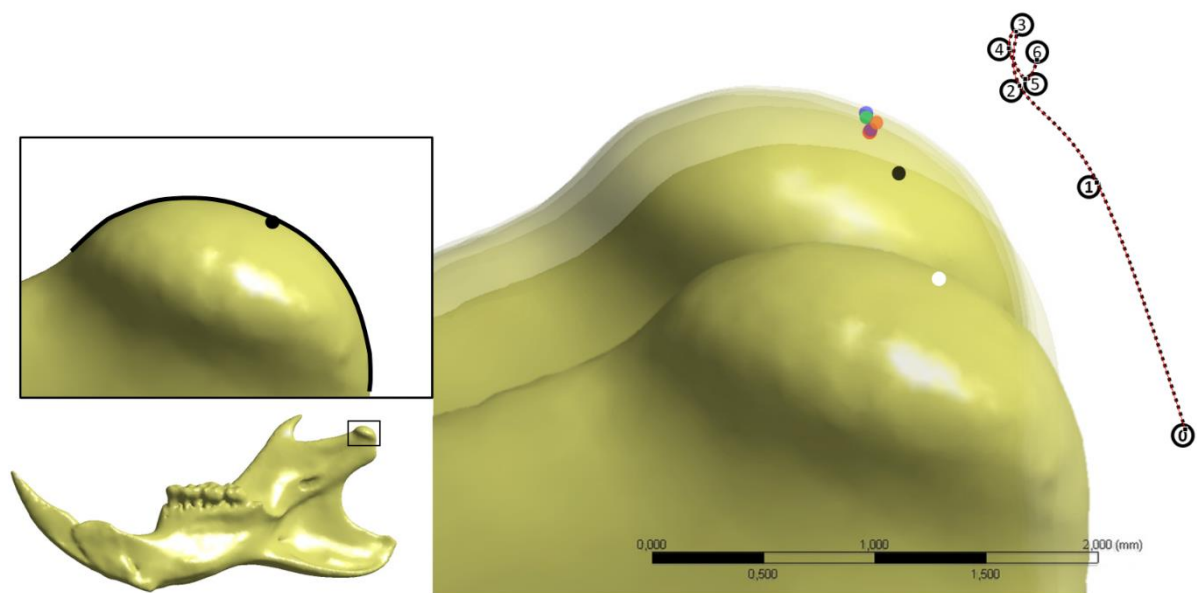


Figure 5. Position of right condyle (medial view) from the initial condition (unloaded model) and the six phases of power stroke cycle. The black point on the left indicates the point selection on the highest point of the condyle curvature. The colored points on the right side indicate each phase of power stroke cycle: White (Initial condition – unloaded model); Black point (Phase 1); Red point (Phase 2); Blue point (Phase 3); Green point (Phase 4); Purple point (Phase 5) and Orange point (Phase 6). The dashed line indicates the orientation of position of condyle from the initial condition (point number 0) to the last phase (point number 6).

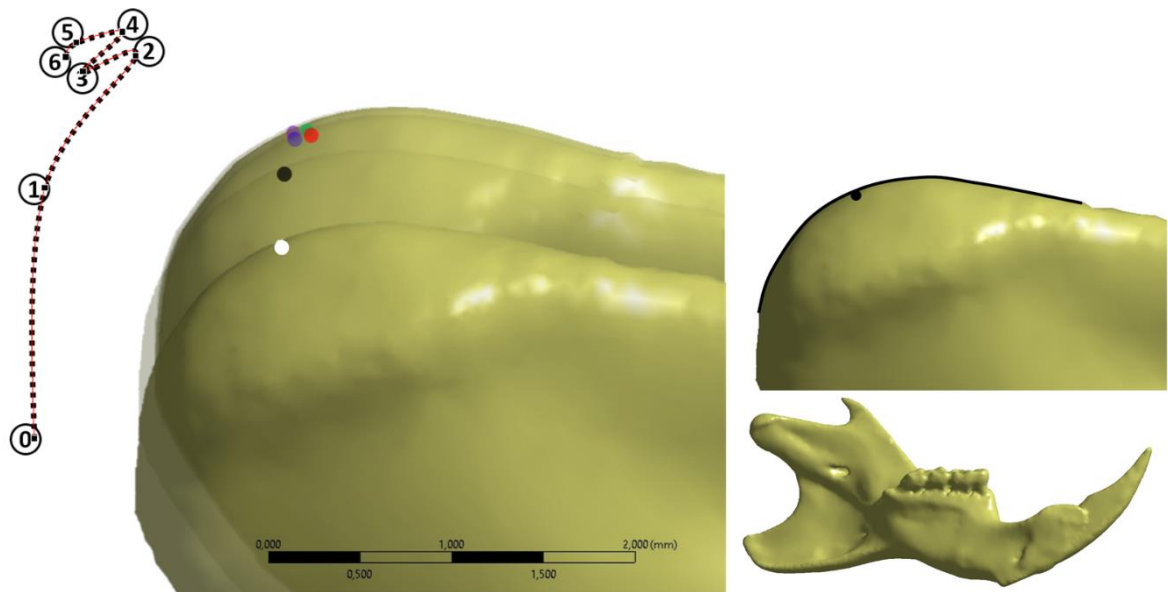


Figure 6. Position of left condyle (medial view) from the initial condition (unloaded model) and the six phases of power stroke cycle. The black point on the left indicates the point selection on the highest point of the condyle curvature. The colored points on the right side indicate each phase of power stroke cycle: White (Initial condition – unloaded model); Black point (Phase 1); Red point (Phase 2); Blue point (Phase 3); Green point (Phase 4); Purple point (Phase 5) and Orange point (Phase 6). The dashed line indicates the orientation of position of condyle from the initial condition (point number 0) to the last phase (point number 6).

DISCUSSION

This study presented a computational simulation using the FEM based on the effects of masticatory muscle on the Wistar rat mandible, described by Weijs and Dantuma (1975). The simulation was carried out specifically to reproduce the 6 phases of the power stroke, characterized by the molar action on the food particles. The description proposed by Weijs and Dantuma (1975) presents kinematic parameters from data obtained by electromyography and x-ray cinematographic films. The FEM simulation in our study featured a static structural analysis, which presented the data from the total deformation of the mandible after muscle actions in the different phases of the power stroke. Although the methods are different, this simulation allows to apply the mandibular pattern in the power stroke phases since the closed mouth position (Weijs and Dantuma, 1975) features the deformation instead movements. The molar chewing process under static conditions has been simulated previously by FEM, which

resulted in stress and, consequently, bone deformations in the mandible (Tsouknidas et al., 2017; Buezas et al., 2019), allowing the study of the mechanical behavior of the mandible successfully.

Differently from the study by Weijs and Dantuma (1975), which obtained muscle force data from electromyography, this study used a method similar to previous FEM studies for the reproduction of muscle action, using morphological data of the mandibular elevator muscles from microCT associated to iodine-based contrast (Cox et al., 2012; Buezas et al., 2019), and the calculation of the estimated muscle force from the CSA. This method was previously used to simulate muscle action in infant mandibles (Humphries et al., 2021), which was used as a reference for this study. On the other hand, the study by Tsouknidas et al. (2017) used the resultant of muscle forces in two scenarios involving incisal loading (named as gnawing) and molar loading (named as chewing).

Previous studies (Cox et al., 2012; Tsouknidas et al. 2017; Buezas et al., 2019) simulated a linear muscle load to assess the stress distribution on the mandible in rodents. In a novel purpose, this study reproduced the non-linear feature of the muscle actions in the 6 phases of the power stroke (molar chewing) by FEM and, thus, it allows to evaluate the different patterns of mandibular deformation from the variations of the muscular actions in each phase. Such variations were used from the variations of the muscular contraction percentages proposed by Weijs and Dantuma (1975), which has applied in the estimated maximum values of muscle force calculated in our study. These associations support the realistic characteristic of computational models, since the association of experimental with computational data is important for model validation (Rossi et al., 2021).

Our results were evaluated according to the biomechanical response of mandible described by Weijs and Dantuma (1975). According to these authors, the angle between the mandibular rami (named AR in our study) varies during the power stroke phases, which

decreases from large to small angle from the first to the last phase. From the TD of the mandible, the AR values decreased along the 6 phases of the power stroke and, thus, corroborating with described pattern. Although the absolute AR values were not described in the study by Weijs and Dantuma (1975), these authors describe a variation to a very smaller angle in the last phase of the power stroke. Our study presented a lower variation of values (36.93° in phase 1 to 34.55° in phase 6), whose scenario might be associated with the static simulation. Regarding the positioning of the condyle, the study by Weijs and Dantuma (1975) described a transition to an anterior position from the first to the last phase of power stroke. In the anteroposterior direction, our results corroborate with the previously proposed description because, in general, the final position of the condyle in this axis was anterior in relation to the first phase. However, our results showed low variations as seen in figures 7 and 8. It is suggested that this pattern is associated with the decrease of temporal muscle contraction, whose muscle is closer to the condyle, after phase 2 on the right and left sides. In addition, the superior position of the condyle was also observed, whose result is associated with total deformation in the regions of the middle third of the mandibular ramus (considering the superior-inferior thirds) due to the major influence of the masseter muscle action in these regions. The region of the condylar process is highly subjected to muscle actions during chewing, as observed in the stress distribution in the study by Tsouknidas et al. (2017).

Considering the objectives of this study, computational simulation by FEM was important to apply the biomechanical concepts in a functional approach (Prado et al., 2013; Freire et al., 2014; Prado et al., 2016). However, the difficult to validate finite element models in the simulation of molar chewing in rats occur due to the difficulties in obtaining *in vivo* data. Thus, our study proposed the use of *in vivo* data from previous study (percentage of muscle contraction from electromyographic data) (Weijs and Dantuma, 1975) to make a more realistic computational model. Our study was carried out based on a static structural analysis, which is

considered a limitation in relation to the kinematic data carried out by Weijs and Dantuma (1975). The recent technologies for kinematic studies such as three-dimensional videofluoroscopy associated with dynamic finite element analysis can bring more realistic data for understanding the mandibular biomechanical behavior of rats during mastication.

CONCLUSION

Considering the limitations of computational simulation by FEM, the results presented similar biomechanical pattern in the power stroke phase, in accordance with the described experimentally by Weijs and Dantuma (1975).

ACKNOWLEDGMENTS

This study was financed in part by the Coordenação de Aperfeiçoamento de Pessoal de Nível Superior – Brasil (CAPES) – finance code 001.

REFERENCES

1. Buezas, G.N., Becerra, F., Echeverría, A.I., Cisilino, A., Vassallo, A.I. (2019). Mandible strength and geometry in relation to bite force: a study in three caviomorph rodents. *J Anat.* Apr;234(4):564-575. doi: 10.1111/joa.12946.
2. Cox, P. G., Fagan, M. J., Rayfield, E. J., Jeffery, N. (2011). Finite element modeling of squirrel, guinea pig and rat skulls: using geometric morphometrics to assess sensitivity. *J Anat.* 219: 696-709. doi: 10.1111/j.1469-7580.2011.01436.x.
3. Cox, P. G., Rayfield, E. J., Fagan, M. J., Herrel, A., Pataky, T. C., Jeffery, N. (2012). Functional evolution of the feeding system in rodents. *PLoS One.* 7(4):e36299. doi: 10.1371/journal.pone.0036299.

4. Ferreira, B. C., Freire, A. R., Araujo, R., do Amaral-Silva, G. K., Okamoto, R., Prado, F. B., Rossi, A.C. (2020). β -catenin and its relation to alveolar bone mechanical deformation - a study conducted in rats with tooth extraction. *Front Physiol.* 11:549. doi: 10.3389/fphys.2020.00549.
5. Freire, A. R., Noritomi, P. Y., Rossi, A. C., Prado, F. B., Haiter Neto, F., Caria, P. H. F. (2014). Biomechanics of the Human Canine Pillar Based on its Geometry Using Finite Element Analysis. *Int. J. Morphol.* 32:214-220. doi: 10.4067/S0717-95022014000100036.
6. Haddad, J. (2018). Morphological characteristics of masticatory muscles in Wistar rats (*Rattus norvegicus albinus*) by computed microtomography (DISSERTAÇÃO Mestra em Biologia Buco-Dental). Piracicaba, SP. doi: 10.47749/T/UNICAMP.2018.1045615
7. Hiimäe, K. M., Ardran, G.M. A cinefluorographic study of mandibular movement during feeding in the rat (*Rattus norvegicus*). (1968). *J. Zool. (London)*. 154: 139-154. doi: 10.1111/j.1469-7998.1968.tb01654.x
8. Hiimäe, K., Houston, W. J. B. (1971). The structure and function of the jaw muscles in the rat (*Rattus norvegicus* L.) I. Their anatomy and internal architecture. *J. Zool. (London)*. 50(1):75-99. doi: 10.1111/j.1096-3642.1971.tb00753.x
9. Humphries, L. S., Reid, R. R., Ross, C. F., Taylor, A. B., Collins, J. M., Freire, A. R., Rossi, A. C., Prado, F. B. (2021). Biomechanical and morphological analysis of Pierre Robin sequence mandible: Finite element and morphometric study. *Anat Rec (Hoboken)*. 304(7):1375-1388. doi: 10.1002/ar.24543.
10. Kaku, M., Uoshima, K., Yamashita, Y., Miura, H. (2005). Investigation of periodontal ligament reaction upon excessive occlusal load – osteopontin induction among periodontal ligament cells. *J Periodont Res.* 40: 59-66. doi: 10.1111/j.1600-0765.2004.00773.x.
11. Prado, F. B., Freire, A. R., Rossi, A. C., Ledogar, J. A., Smith, A. L., Dechow, P. C., Strait, D. S., Voigt, T., Ross, C. F. (2016). Review of In Vivo Bone Strain Studies and Finite

Element Models of the Zygomatic Complex in Humans and Nonhuman Primates: Implications for Clinical Research and Practice. *Anat Rec (Hoboken)*. 299(12):1753-1778. doi: 10.1002/ar.23486.

12. Prado, F. B., Noritomi, P. Y., Freire, A. R., Rossi, A. C., Haiter Neto, F., Caria, P. H. F. (2013). Stress Distribution in Human Zygomatic Pillar Using Three-Dimensional Finite Element Analysis. *Int. J. Morphol.* 31:1386-1392. doi: 10.4067/S0717-95022013000400038.

13. Rossi, A. C., Freire, A. R., Ferreira, B. C., Faverani, L. P., Okamoto, R., Prado, F. B. (2021). Effects of premature contact in maxillary alveolar bone in rats: relationship between experimental analyses and a micro scale FEA computational simulation study. *Clin Oral Investig.* 25(9):5479-5492. doi: 10.1007/s00784-021-03856-1.

14. Rossi, A. C., Freire, A. R., Prado, F. B., Asprino, L., Correr-Sobrinho, L., Caria, P. H. F. (2014). Photoelastic and finite element analyses of occlusal loads in mandibular body. *Anat Res Int.* 2014:174028. doi: 10.1155/2014/174028.

15. Tanaka, E., Rodrigo, D. P., Tanaka, M., Kawaguchi, A., Shibazaki, T., Tanne, K. (2001). Stress analysis in the TMJ during jaw opening by use of a three-dimensional finite element model based on magnetic resonance images. *Int J Oral Maxillofac Surg.* 30(5): 421-30. doi: 10.1054/ijom.2001.0132.

16. Tsouknidas, A., Jimenez-Rojo, L., Karatsis, E., Michailidis, N., Mitsiadis, T.A. (2017). A Bio-Realistic Finite Element Model to Evaluate the Effect of Masticatory Loadings on Mouse Mandible-Related Tissues. *Front Physiol* May 9;8:273. doi: 10.3389/fphys.2017.00273.

17. Weijs, W. A., Dantuma, R. (1975). Electromyography and Mechanics of Mastication in the Albino Rat. *J Morphol.* 146: 1-34. doi: 10.1002/jmor.1051460102.

18. Watson, P. J., Gröning, F., Curtis, N., Fitton, L. C., Herrel, A., McCormack, S. W., Fagan, M. J. (2014). Masticatory biomechanics in the rabbit: a multi-body dynamics analysis. *J R Soc Interface.* 11(99):20140564. doi: 10.1098/rsif.2014.0564.

3 CONCLUSÃO

A partir dos objetivos propostos e, considerando as limitações da análise de elementos finitos, os resultados deste estudo demonstraram computacionalmente o comportamento da estrutura mandibular em acordo com o proposto experimentalmente no estudo de Weijs e Dantuma (1975). Os dados concluem que as variações nas contrações musculares aplicadas no modelo computacional alteram o ângulo entre os ramos da mandíbula e a posição do côndilo durante a fase de mordida molar em ratos da linhagem Wistar.

REFERÊNCIAS*

1. Cox PG, Fagan MJ, Rayfield EJ, Jeffery N. Finite element modeling of squirrel, guinea pig and rat skulls: using geometric morphometrics to assess sensitivity. *J Anat.* 2011, 219: 696-709.
2. Cox PG, Rayfield EJ, Fagan MJ, Herrel A, Pataky TC, Jeffery N. Functional evolution of the feeding system in rodents. *PLoS One.* 2012;7(4):e36299.
3. Ferreira BC, Freire AR, Araujo R, do Amaral-Silva GK, Okamoto R, Prado FB, Rossi AC. β -catenin and its relation to alveolar bone mechanical deformation - a study conducted in rats with tooth extraction. *Front Physiol.* 2020; 11:549.
4. Freire AR, Noritomi PY, Rossi AC, Prado FB, Haiter Neto F, Caria PHF. Biomechanics of the Human Canine Pillar Based on its Geometry Using Finite Element Analysis. *International Journal of Morphology (Online)*, 2014; 32:214-220.
5. Hiiemäe KM, Ardran GM. A cinefluorographic study of mandibular movement during feeding in the rat (*Rattus norvegicus*). *J. Zool. (London)*. 1968; 154: 139-154.
6. Hiiemäe KM, Houston WJB. The structure and function of the jaw muscles in the rat (*Rattus norvegicus* L.) I. Their anatomy and internal architecture. *Zoological Journal of the Linnean Society.* 1971; 50(1):75-99
7. Kaku M, Uoshima K, Yamashita Y, Miura H. Investigation of periodontal ligament reaction upon excessive occlusal load – osteopontin induction among periodontal ligament cells. *J Periodont Res.* 2005; 40: 59-66.
8. Prado FB, Freire AR, Cláudia Rossi A, Ledogar JA, Smith AL, Dechow PC, Strait DS, Voigt T, Ross CF. Review of In Vivo Bone Strain Studies and Finite Element Models of the Zygomatic Complex in Humans and Nonhuman Primates: Implications for Clinical Research and Practice. *Anat Rec (Hoboken)*. 2016; 299(12):1753-1778.
9. Prado FB, Noritomi PY, Freire AR, Rossi AC, Haiter Neto F, Caria PHF. Stress Distribution in Human Zygomatic Pillar Using Three-Dimensional Finite Element Analysis. *International Journal of Morphology (Online)*. 2013; 31:1386-1392.
10. Rossi AC, Freire AR, Ferreira BC, Faverani LP, Okamoto R, Prado FB. Effects of premature contact in maxillary alveolar bone in rats: relationship between experimental analyses and a micro scale FEA computational simulation study. *Clin Oral Investig.* 2021; 25(9):5479-5492.

*De acordo com as normas da UNICAMP/FOP, baseadas na padronização do International Committee of Medical Journal Editors – Vancouver Group. Abreviatura dos periódicos em conformidade com o PubMed.

11. Rossi AC, Freire AR, Prado FB, Asprino L, Correr-Sobrinho L, Caria PH. Photoelastic and finite element analyses of occlusal loads in mandibular body. *Anat Res Int.* 2014; 2014:174028.
12. Watson PJ, Gröning F, Curtis N, Fitton LC, Herrel A, McCormack SW, Fagan MJ. Masticatory biomechanics in the rabbit: a multi-body dynamics analysis. *J R Soc Interface.* 2014; 11(99):20140564.
13. Weijjs WA, Dantuma R. Electromyography and Mechanics of Mastication in the Albino Rat. *J Morphol.* 1975, 146: 1-34.

ANEXO 1: COMPROVANTE DE SUBMISSÃO NA REVISTA

Journal of Morphology Research Article	
COMPUTATIONAL ANALYSIS OF THE MECHANICAL BEHAVIOR OF MANDIBULAR BONE STRUCTURES DURING THE MOLAR POWER STROKE PHASE IN WISTAR RATS	
Submission Status	Submitted
Submitted On	16 November 2022 by ALEXANDRE FREIRE
Submission Started	15 November 2022 by ALEXANDRE FREIRE

This submission has been sent to the editorial office and cannot be edited. Further instructions will be emailed to you from Manuscript Central.

[View Submission Overview](#)

Need help choosing a journal?
We've put together some resources and tools to help you find the right journal for your research.

[Find a Journal](#)

ANEXO 2: COMPROVANTE DO COMITÊ DE ÉTICA EM PESQUISA



Comissão de Ética no Uso de Animais
CEUA/Unicamp



CEUA/Unicamp

INFORMAÇÃO

A Comissão de Ética no Uso de Animais da UNICAMP – CEUA/UNICAMP – esclarece que não há necessidade de submeter o projeto de pesquisa “ANÁLISE COMPUTACIONAL DO COMPORTAMENTO MECÂNICO DAS ESTRUTURAS ÓSSEAS MANDIBULARES DURANTE A FASE DE MORDIDA MOLAR EM RATOS DA LINHAGEM WISTAR”, de responsabilidade da Profa. Dra. Ana Cláudia Rossi e dos executores: Juliana Haddad, Felipe Bevilacqua Prado e Alexandre Rodrigues Freire, para análise desta comissão.

Justifica-se por se tratar de um projeto que utilizará imagens microtomográficas (microCT) obtidas dos ratos dos grupos controle e experimental já realizadas no protocolo original (protocolo CEUA/UNICAMP – número 4401-1). Não haverá manipulação *in vivo* na Unicamp para este projeto.

Campinas, 24 de maio de 2022.

Prof. Dr. Wagner José Fávaro
Presidente
CEUA/UNICAMP

Rosângela dos Santos
Secretária Executiva
CEUA/UNICAMP

CEUA/UNICAMP
Rua Monteiro Lobato, 80
13083-970 Campinas, SP – Brasil

Telefone: (19) 3521-6369
E-mail: comisib@unicamp.br
https://www.ib.unicamp.br/comissoes/ceua_principal

Documento assinado. Verificar autenticidade em sigad.unicamp.br/verifica
Informar código CD81D962 1A9C47C1 8DD053E4 40374C8F

Documento assinado eletronicamente por **WAGNER JOSE FAVARO, PRESIDENTE DA CEUA/UNICAMP**, em 26/05/2022, às 17:44 horas, conforme Art. 10 § 2º da MP 2.200/2001 e Art. 1º da Resolução GR 54/2017.

Documento assinado eletronicamente por **ROSANGELA DOS SANTOS, SECRETÁRIA EXECUTIVA CEUA/UNICAMP**, em 26/05/2022, às 09:40 horas, conforme Art. 10 § 2º da MP 2.200/2001 e Art. 1º da Resolução GR 54/2017.



A autenticidade do documento pode ser conferida no site:
sigad.unicamp.br/verifica, informando o código verificador:
CD81D962 1A9C47C1 8DD053E4 40374C8F



ANEXO 3: COMPROVANTE DO SOFTWARE ANTI-PLÁGIO

ANÁLISE COMPUTACIONAL DO COMPORTAMENTO MECÂNICO DAS ESTRUTURAS ÓSSEAS MANDIBULARES DURANTE A FASE DE MORDIDA MOLAR EM RATOS DA LINHAGEM WISTAR

RELATÓRIO DE ORIGINALIDADE

6%
ÍNDICE DE SEMELHANÇA

5%
FONTES DA INTERNET

5%
PUBLICAÇÕES

1%
DOCUMENTOS DOS ALUNOS

FONTES PRIMÁRIAS

1	Bram B. J. Merema, Jelbrich J. Sieswerda, Frederik K. L. Spijkervet, Joep Kraeima, Max J. H. Witjes. "A Contemporary Approach to Non-Invasive 3D Determination of Individual Masticatory Muscle Forces: A Proof of Concept", Journal of Personalized Medicine, 2022 Publicação	1%
2	justinledogar.weebly.com Fonte da Internet	1%
3	www.ncbi.nlm.nih.gov Fonte da Internet	1%
4	archive-ouverte.unige.ch Fonte da Internet	1%
5	repositorio.ufc.br Fonte da Internet	<1%